EurJIC
European Journal of Inorganic Chemistry

Research Article
doi.org/10.1002/ejic.202200261

Chemistry Europe
European Chemical Societies Publishing

www.eurjic.org

# Single- *vs* Double-Decker Copper 12-MC-4 Metallacrown Using the Coordination Flexibility of a Soft Donor Ligand

Christoph Gamer,[a] Sriram Sundaresan,[a] Luca M. Carrella,[a] and Eva Rentschler*[a]

2-Methylmercaptobenzohydroxamic acid (**mmbHA**) has been synthesized and used to form $\{Cu^{II}Cl_2(MeOH)[12\text{-}MC_{Cu(II)N(mmbHA)}\text{-}4]\}_2\cdot 4MeOH$ (**1**) and $\{Cu^{II}(\mu_2\text{-}ClO_4)(MeOH)_2(py)_4[12\text{-}MC_{Cu(II)N(mmbHA)}\text{-}4]\}ClO_4$ (**2**), a copper(II) based double-decker and a discrete metallacrown (MC) system, respectively. While **1** forms in the absence of a coordinating co-ligand, the presence of pyridine (Py) leads to a change in the coordination mode of **mmbHA** and a discrete MC **2** is formed. Both compounds have been structurally and magnetically characterized. The magnetic susceptibility measured from 2–300 K shows overall antiferromagnetic exchange coupling within both crown structures and the obtained coupling constants are $J_1 = -88.0(1)\ cm^{-1}$ and $J_2 = -64.7(3)\ cm^{-1}$ for **1** and $J_1 = -90.0(5)\ cm^{-1}$ and $J_2 = -31.1(1)\ cm^{-1}$ for **2**. However, the ratio of the coupling parameters is highly affected by the structural change.

## Introduction

Since metallacrowns (MC) were first introduced in 1989 by Pecoraro, they have been of great interest in various fields of research including molecular recognition, host-guest chemistry, catalysis, magnetism and luminescence.[1–6] Like their organic analogues crown ethers MC have –[M–N–O]$_n$- repeating units of metal ions, nitrogen and oxygen atoms leading to different ring sizes and enabling MC to coordinate guest metal ions. The most common crown types are 9-MC-3, 12-MC-4 and 15-MC-5.[3–6] Focusing on the 12-MC-4 structural unit (Scheme 1), the ring consists of twelve atoms with four of them being oxygen or nitrogen atoms capable to bind an additional central metal ion. Salicylhydroxamic acid has become the most investigated ligand for the synthesis of MCs.[5,7] Benzohydroxamic acid molecules with donor functionalities in *ortho* position represent a tetradentate ligand system with an ideal constitution for the formation of 12-MC-4 structures. The equatorial coordination environment of the crown forming metal ions, M (in Figure 1), is set up by a $NO_2X$ donor set, while the central metal ion exhibits a $O_4$ environment. Variation of the donor atom X leads to a change in the ligand field strength and affects the coordination affinity towards the ring-forming metal ions. Hence, it is possible to rationally design a MC ligand system which will be able to form heterometallic MCs. Their self-assembly synthesis procedure makes a high selectivity of the coordination pockets inevitable, especially for 3d metal MC systems. The central cavity needs to offer a different coordination affinity, in contrast to the outer crown pocket, in order to be able to synthesize heterometallic MCs. So far, only two heterobimetallic MC are

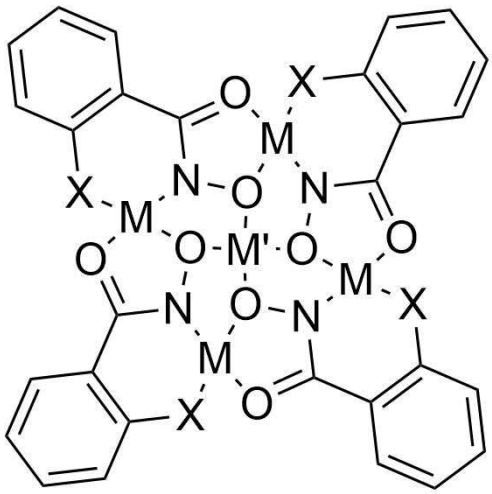

**Scheme 1.** Schematic representation of a 12-MC-4 structure based on benzohydroxamic acid ligand molecules with donor functionalities in *ortho* position.

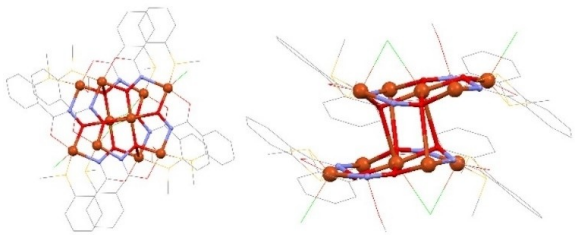

**Figure 1.** Top (left) and side view (right) of the MC double-decker $\{Cu^{II}Cl_2(MeOH)[12\text{-}MC_{Cu(II)N(mmbHA)}\text{-}4]\}_2\cdot 4MeOH$ (**1**). Colour code: Orange – Cu-(II), red – oxygen, blue – nitrogen, yellow – sulfur, gray – carbon, green – chlorine.

[a] *Dr. C. Gamer, Dr. S. Sundaresan, Dr. L. M. Carrella, Prof. E. Rentschler*
*Department of Chemistry, Johannes-Gutenberg University*
*Duesbergweg 10–14, 55128 Mainz, Germany*
*E-mail: rentschler@uni-mainz.de*

*Supporting information for this article is available on the WWW under https://doi.org/10.1002/ejic.202200261*

Research Article
doi.org/10.1002/ejic.202200261



reported. Some of us in 2014 reported the first copper centered iron [$Fe_4Cu$] MC[8] and more recently Zaleski and co-workers reported a 12-MC-4 heterobimetallic Cu–Mn MC.[9] For the former example the greater coordination affinity of the hydroxamic acid moiety towards $Fe^{3+}$ ions than $Cu^{2+}$ ions is the key fact of this rare MC complex. Thus, while the 12-MC-4 crown is formed by six-coordinated iron ions, it provides a square planar coordination pocket that is well suited for a $Cu^{2+}$ ion.

However, this attempt to form heterometallic MCs is solely focused on the coordination affinity of the central MC cavity. The purpose of the present work is to study a more rational approach for the implementation of softer metal ions in the crown by increasing the ligand's donor affinity towards softer crown forming metal ions. This has been achieved by introducing a sulfur donor atom in the metallacrown ligand system. A direct change from the hydroxyl group in salicylhydroxamic acid to the thiol group results in the trivalent thiosalicylhydroxamic acid. However, it is known that under common reaction conditions for the synthesis of an *ortho* functionalized benzohydroxamic acid, the sulfur derivative undergoes a cyclization reaction yielding 1,2-benzisothiazolin-3-one.[10] Hence, the reactive thiol group has been protected by methylation leading to the divalent 2-methylmercapto-benzohydroxamic acid (**mmbHA**). To investigate the ability of this ligand to form 12-MC-4 complexes, two novel homometallic Cu(II) complexes have been characterized. The synthesis of the sulfur containing ligand and two copper MC complexes along with the structural and magnetic properties are reported and discussed in detail.

## Results and Discussion

### Synthesis

2-Methylmercaptobenzohydroxamic acid (**mmbHA**) has been synthesized using a three-step synthetic procedure (Scheme 2). In the first step, the esterification of 2-mercaptobenzoic acid was followed by a methylation of the thiol group yielding 2-methylmercaptobenzoic acid methyl ester. The commonly used substitution reaction with hydroxylamine afforded the final hydroxamic acid **mmbHA** in moderate yields. The successful ligand formation was confirmed by $^{1}$H-NMR and $^{13}$C-NMR.

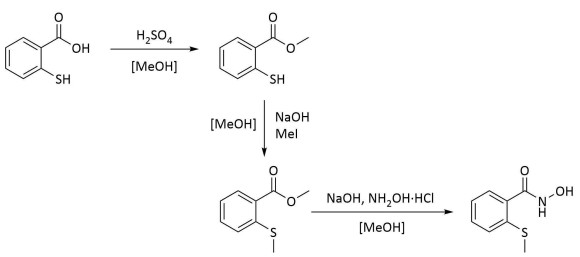


**Scheme 2.** Three step reaction procedure for the synthesis of 2-methylmercaptobenzohydroxamic acid (**mmbHA**).

The reaction of the ligand with a Cu(II) salt, led to the formation of the complexes in crystalline form in both the cases. Complex (**1**) was isolated as green crystals with the formula $\{Cu^{II}Cl_2(MeOH)[12\text{-}MC_{Cu(II)N(mmbHA)}\text{-}4]\}_2\cdot 4MeOH$ from reaction of **mmbHA** and copper(II) chloride in methanol, after two days, with triethylamine as a base. The discrete copper MC $\{Cu^{II}(\mu_2\text{-}ClO_4)(MeOH)_2(py)_4[12\text{-}MC_{Cu(II)N(mmbHA)}\text{-}4]\}ClO_4$ (**2**) was isolated as green crystalline solid upon the reaction of copper(II) perchlorate, pyridine (py) and manganese(II) pivalate in methanol after a week of slow evaporation. While neither the manganese ions nor any pivalate counterions are present in the crystal structure of compound **2**, the complexation was however unsuccessful in the absence of the manganese(II) pivalate. To probe the role of Mn(II) and pivalate ions, the reaction has been carried out replacing the manganese salt by copper(II) pivalate or potassium pivalate. Isolation of **2** was not possible in both the attempts.

### Crystal Structures

Complex **1**: The crystallographic unit cell of the triclinic space group $P\bar{1}$ consists of two fused homometallic copper MCs and four non-coordinating methanol molecules. Both planes of the double-decker MC are shifted towards each other, allowing only two copper ions of each crown to be axially coordinated by oxygen atoms from the adjacent plane (Figure 1).

The asymmetric unit of complex **1** (Figure 2) consists of four **mmbHA** ligand molecules and five Cu(II) ions with additional two chloride ions and one methanol molecule coordinating out of plane. The central metal ion (Cu1) of each MC is embedded in a distorted octahedral coordination environment. The four hydroxamato oxygen atoms of the ligands occupy the

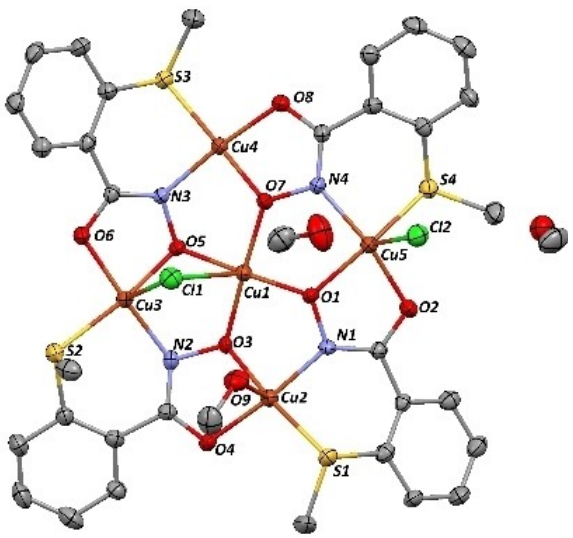


**Figure 2.** Asymmetric unit of the crystal structure of compound **1**. ORTEP representation with atomic displacement parameters at 50% level of probability. Hydrogen atoms have been omitted for clarity. Colour code: Orange – Cu(II), red – oxygen, blue – nitrogen, yellow – sulfur, grey – carbon, green – chlorine.

Research Article
doi.org/10.1002/ejic.202200261



equatorial coordination sites of Cu1. One chloride ion (Cl1) and another hydroxamato oxygen atom (O5) from a neighboring MC plane fill the axial positions of the octahedral environment. The peripheral metal ions are fivefold coordinated within a distorted square pyramidal geometry. The two distinct binding pockets of **mmbHA** form the equatorial $NSO_2$ donor set. Two chloride ions (Cl1, Cl2) and two oxygen atoms (O3, O9) occupy the axial coordination sites of Cu3, Cu5, Cu4 and Cu2, respectively. Cl1 forms a μ-bridge between the central Cu1 and the peripheral Cu3. Cl2 is only axially coordinated to the peripheral Cu5 ion. While O9 and O3 are coordinating methanol molecule and hydroxamato oxygen atom of the neighboring MC plane respectively.

The Cu–Cu distances from the central guest ion to the crown forming metal ions varies from 3.058 Å for Cu1–Cu3 up to 3.291 Å for Cu1–Cu5. The distances of the N–O bridged ring metal ions slightly vary from 4.428 Å for Cu2–Cu3 up to 4.597 Å for Cu2–Cu5. The two available $\mu_2$-O-bridged Cu–Cu inter MC distances are 3.496 Å for Cu1–Cu1′ and 3.855 Å for Cu1–Cu4′. Detailed overview of the atom-atom distances and bond length present in complex **1** is summarized in Table S2. The Cu1–O-(hydroxamato)–$Cu_{crown}$ angles within one MC plane are 113.04° (Cu1–O3–Cu2), 100.63° (Cu1–O5–Cu3), 117.80° (Cu1–O7–Cu4) and 116.06° (Cu1–O1–Cu5). This tremendous discrepancy of one of the four angles is caused by the bridging $\mu_2$–Cl ligand provoking a bending of the MC plane. This structural deformation is also represented by a strong deviation of two of the Cu–N–O–Cu torsion angles from the ideal 180° (Table S2). In addition to this, in compound **1**, the C14–C15–S2–C16 torsion angle of 101.15° indicating a nearly perpendicular orientation of the methyl group towards the ligands benzyl plane. The other three methyl groups show a more in plane orientation (Figure S12). This conformation might be due to a non-classical hydrogen bond from C16 towards an adjacent methanol molecule (O10).

Complex **2**: Single crystal X-ray diffraction revealed that compound **2** crystallizes in tetragonal crystal system in $I\bar{4}$ space group with one MC per unit cell. The homometallic copper MC is formed by four **mmbHA** molecules, five copper(II) ions, four pyridine and three methanol molecules. To balance the charge, there are two perchlorates found within the unit cell, one coordinating and another non-coordinating (Figure 3). However, the asymmetric unit (Figure S3) consists of only two crystallographically independent copper ions, the central metal ion Cu1 and the crown forming peripheral metal ion Cu2. The Cu1 ion is located on a center of inversion of a fourfold inversion axis. Cu1 exhibits a square pyramidal coordination environment which is formed by four symmetry generated hydroxamato oxygen atoms (O1) and an additional axial oxygen atom (O9) from a coordinating perchlorate ion.

The ring-forming copper ions (Cu2) are also embedded in a square pyramidal coordination environment. The axial coordination site is occupied by a perchlorate oxygen atom (O11) for one Cu(II) center or by coordinating methanol molecules (O8) in the remaining three Cu(II) ions. In contrast to the MC structure of compound **1** the methylated mercapto sidearm, S1, does not coordinate and remains uncoordinated. A greater donor

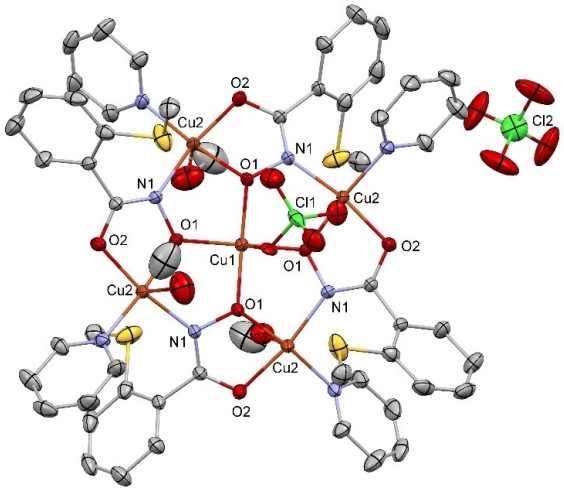


**Figure 3.** Molecular structure of $Cu^{II}(\mu_2\text{-}ClO_4)(MeOH)_2(py)_4$ [12-$MC_{Cu(II)N(mmbHA)^-}$4]$ClO_4$ (**2**). ORTEP representation with atomic displacement parameters at 50% level of probability. The methyl group at S1 is disordered over two positions with a placement ratio of 50:50. The disorder and Hydrogen atoms have been omitted for clarity. Colour code: Orange – Cu(II), red – oxygen, blue – nitrogen, yellow – sulfur, grey – carbon, green – chlorine.

strength leads the pyridine molecules to coordinate preferably in-plane than in axial position. In contrast to the $NO_2S$ environment for the peripheral Cu(II) ions, the equatorial coordination environment of the ring-forming metal ions consists of a $N_2O_2$ donor set in *cis* conformation. This coordination mode is known from anthranilic hydroxamic acid (and derivatives) based copper MCs.[11,12]

The Cu2–S distance at 3.2653 Å is indicative for a very long Jahn-Teller axis. Hence, the coordination environment for all crown-forming copper ions could also be described as distorted octahedral with an elongated S1–Cu2–O8 axis.

The Cu1–Cu2 distance of 3.257 Å is slightly larger than the average value of the distances between the central and the ring metal ions found in compound **1** (3.206 Å). A Cu–N–O–Cu torsion angle of 174.53° supports the planar MC structure, especially in contrast to the averaged torsion angle of compound **1** (156.78°). A Cu1–O1–Cu2 bond angle of 116.20° is observed. The MC plane is separated from the next neighboring one by around 10 Å with a stacked arrangement along the crystallographic c-axis (see Figure S14). The parallel orientation of the pyridine co-ligand towards the benzyl plane of the neighboring **mmbHA** ligand (see Figure 4) indicates π–π stacking of the aromatic ring systems.

## Magnetic Properties

Compounds **1** and **2** have been magnetically characterized by temperature-dependent susceptibility measurements (Figure 5). The data of complex **1** was evaluated for a single metallacrown with a molar mass of M(**1**)/2 = 1209 g mol$^{-1}$. It has been shown, that the intermolecular exchange between the two MCs will have only a very minor effect due to the axial-equatorial

Research Article
doi.org/10.1002/ejic.202200261



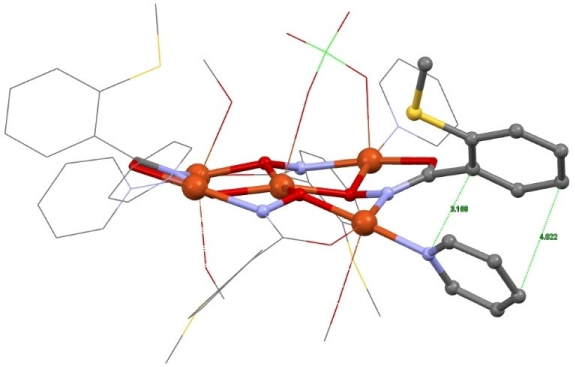

**Figure 4.** Parallel orientation of the aromatic ring systems of **mmbHA** and the pyridine co-ligand in **2**. The methyl group at S1 is disordered over two positions with a placement ratio of 50:50. Colour code: Orange – Cu(II), red – oxygen, blue – nitrogen, yellow – sulfur, grey – carbon, green – chlorine.

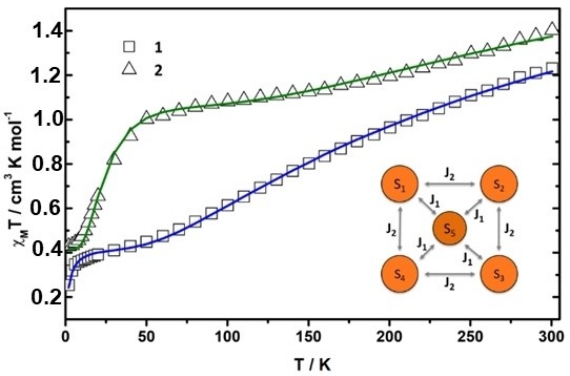


**Figure 5.** Temperature dependent magnetic behaviour of compounds **1** and **2** and the best fit (solid line) of the intramolecular magnetic coupling, $J_1$ and $J_2$ using the star-like coupling scheme for 12-MC-4 structures (inlet).

bridging mode between the Cu(II) centers by adding a mean field parameter (*zJ*, Equation S1 in ESI). The characteristic magnetic behavior of MC compounds is based on their intramolecular exchange coupling.[6,13] Additionally, this approach leads to an easier comparison of the magnetic behavior of both compounds and other copper(II) based 12-MC-4 structures in the literature. The commonly used coupling scheme to consider the intramolecular interaction of 12-MC-4 structures is shown in Figure 5 (inlet). Two different coupling pathways are assigned according to the star-like scheme: the radial exchange coupling, $J_1$, between the central metal ion an the peripheral and the tangential coupling within the crown, $J_2$. The exchange Hamiltonian for this coupling behavior can be described as

$$\hat{H}_{ex}(MC) = -2J_1\hat{S}_5\left(\hat{S}_1+\hat{S}_2+\hat{S}_3+\hat{S}_4\right) - 2J_2(\hat{S}_1\hat{S}_2+\hat{S}_2\hat{S}_3+\hat{S}_3\hat{S}_4+\hat{S}_4\hat{S}_1).$$

For complex **1** the product of magnetic susceptibility and temperature reaches a value of 1.23 $cm^3$ K $mol^{-1}$ at 300 K, which is far below the expected spin-only value for five uncoupled Cu(II) ions (1.875 $cm^3\,K\,mol^{-1}$). This observation accompanied by a steep decrease of the $\chi_M T$ product upon cooling down the sample indicates a dominating antiferromagnetic exchange coupling. At temperatures between 40 K and 10 K the curve reaches a plateau of 0.43 $cm^3$ K $mol^{-1}$ and starts decreasing again at very low temperatures. The plateau suggests the presence of a spin ground state of S = 1/2 ($\chi_M T_{theo}(S=1/2)$ = 0.375 $cm^3\,K\,mol^{-1}$), expected for a homometallic antiferromagnetically coupled copper MC.[8] The decrease below 10 K is commonly observed in compounds undergoing weak intermolecular exchange coupling. The best fit result of the magnetic data of **1** was obtained using the program PHI[14] leading to $J_1$ = −88.0(1) $cm^{-1}$, $J_2$ = −64.7(3) $cm^{-1}$, g($Cu^{2+}$) = 2.146(2) and $zJ$ = −0.944(52) $cm^{-1}$ (R = $2.55\cdot10^{-3}$). The error of the fit routine (R) is calculated according to the sum of squares approach. These values are in very good agreement with the literature.[15–18]

For compound **2** a slightly different magnetic behavior is observed. The $\chi_M T$ product decreases from 1.40 $cm^3\,K\,mol^{-1}$ at 300 K very gradually until 50 K and reaches a plateau at a value of 1.1 $cm^3\,K\,mol^{-1}$. At lower temperatures $\chi_M T$ product rapidly decreases to 0.43 $cm^3\,K\,mol^{-1}$ at 2 K as the antiferromagnetic exchange coupling dominates. The magnetic data was fitted using PHI applying the same coupling scheme (Figure 5, inset). The resulting fit yielded $J_1$ = −90.0(5) $cm^{-1}$, $J_2$ = −31.1(1) $cm^{-1}$ and g($Cu^{2+}$) = 2.111(3) (R = $10.3\cdot10^{-3}$). Noteworthy, the ratio of both coupling parameters $J_1/J_2$ = 2.9 is much higher than observed in compound **1** ($J_1/J_2$ = 1.3).

According to the fit results, the radial exchange $J_1$ seems to be unaffected while the tangential exchange coupling constants $J_2$ differ strongly. For manganese-based 12-MC-4 structures, Song and co-workers[18] stated that a decrease in tangential coupling can be attributed to an increase in the M–N–O–M torsion angle within the crown. This expected relationship is not apparent here. While for complex **2** the torsion angle Cu2–N1–O1–Cu2 of 174.5° hardly deviates from 180° for a completely planar arrangement, and also the sum of all angles at the oxygen donor atom O1 of 347.4° is close to the theoretical value of 360° for planar coordination, this is only partially the case for the comparable angles in complex **1** (Table S2). It should therefore be recalled that the two metallacrown structures differ here by their equatorial donor sets. Replacing the softer and more polarisable sulfur donor atom with a hard nitrogen donor leads to a decrease in electron density in the outer ring of the MC and could therefore lead to a weakening of the tangential coupling as observed in complex **2**. The higher coupling constant ratio $J_1/J_2$ is accompanied by a lowering of the first excited quartet state. While in compound **1** only the third excited state represents a quartet state ($\Delta E_3 \approx 170\ cm^{-1}$), the first excited state in compound **2** is already a quartet state ($\Delta E_1 \approx 35\ cm^{-1}$), as shown in Figure S15. However, the ground state is clearly a doublet state, which is predicted by simple calculations up to a ratio close to 4 (Figure S16).

## Conclusions

Herein, we have reported the synthesis of methylmercaptobenzo hydroxamic acid (**mmbHA**) ligand. It was shown that this ligand is suitable to form 12-MC-4 structures. Two distinct copper(II) based MC systems were synthesized and

Research Article
doi.org/10.1002/ejic.202200261



structurally analyzed. The use of pyridine as co-ligand led to a drastic change of the **mmbHA** coordination mode and thus to the formation of a discrete MC in the case of **2**, whereas a double-decker structure is formed in compound **1**. The temperature dependent magnetic behavior of both complexes were investigated by SQUID magnetometry. The two copper(II) MC complexes represent the first indication that ligand **mmbHA** is able to coordinate softer metal ions. Ongoing work is focused to rationally implement even softer 4d metal ions such as Cd(II) ions into the MC framework using **mmbHA** in order to expand the variety of luminescent MC compounds.

## Experimental Section

### General Information

All used chemicals were commercially available and have been used without further purification. Manganese pivalate was synthesized by dissolving the corresponding carbonate salt in pivalic acid and heating up the reaction mixture. Cooling down to room temperature yielded the crystallized pivalate salt. Infrared spectra have been recorded on a Nicolet 5700 FT-IR-Spectrometer with an attached Smart Orbit ATR (Diamond) probe head from Thermo Electron Cooperation. The background has been measured prior to the samples and is subtracted from the spectra. The measurement range was from 400–4000 $cm^{-1}$. The spectra were averaged over 32 measurements and baseline corrected using the software Omnic® (7.3) from Thermo Electron Cooperation. Magnetic susceptibility studies were obtained on a Quantum Design MPMS-XL SQUID magnetometer in a temperature range from 2 to 300 K. Crystalline samples were filled in a gelatine capsule which was mounted in a plastic straw.[17] Data points have been measured over a length of 4 cm. The volume magnetization derived from the measured response function was corrected by the magnetic contribution of holder and capsule using the julX 1.4.1 program by Bill(26). Including the molar mass of the sample, the molar magnetic susceptibility could be calculated. The diamagnetic contribution of the sample D was taken into account by formula $\chi_D = [(MW)/2)]X10^{-6}$ emu $mol^{-1}$, which results in values very close to those deriving from Pascal's constants.[19] $^1H$ and $^{13}C$-NMR spectra were obtained on a Bruker DRX-400 at room temperature. All compounds were measured in deuterated dimethyl sulfoxide. Chemical shifts were reported in parts per million with the residual solvent peak used as an internal standard (DMSO-$d^6$ = 2.50 ppm for $^1H$ and 39.52 ppm for $^{13}C$). For the analysis of the spectra MestreNova 10.0 was used. Single-crystal X-ray diffraction data (**1** and **2**) were collected on a Bruker Smart APEX II CCD diffractometer. The diffractometer was operated at 45 kV and 35 mA with Mo Kα radiation (λ = 0.71073 Å), and a nitrogen cold stream was applied to keep the collection temperature at 173(2) and 193 K. The structures were solved with ShelXT[20] and refined with ShelXL[21–22] implemented in the program Olex2.[22]

### Ligand synthesis

#### *2-Mercaptobenzoic acid methyl ester*

2-Mercaptobenzoic acid (20 g, 0.130 mol) was suspended in 300 ml methanol and the mixture was cooled to 5 °C under $N_2$ atmosphere. 21 ml sulfuric acid were added dropwise within 5 min. Then the mixture was heated to reflux and stirred overnight. The benzoic acid dissolved under elevated temperatures and the solution became clear and yellow. After 16 h of heating the solution was cooled to room temperature and concentrated under reduced pressure. The reaction mixture was diluted with 200 ml dichloromethane and 200 ml water. The organic layer was separated and successively washed with 100 ml saturated sodium hydrogen carbonate solution and 200 ml brine. After drying over sodium sulphate the solvent was removed under reduced pressure. The resulting residue was purified via fractional distillation. 2-Mercaptobenzoic acid methyl ester was collected at 10 mbar and 120 °C as a light yellow liquid (14.28 g, 84.9 mmol, 65% of theory). $^1H$-NMR (DMSO-$d^6$, 400 MHz, δ (ppm)): 7.90 (dd, 1H, Ar–CH), 7.55 (dd, 1H, Ar–CH), 7.40 (td, 1H, Ar–CH), 7.20 (td, 1H, Ar–CH), 5.29 (s, 1H, SH), 3.83 (s, 3H, $OCH_3$). $^{13}C$-NMR (DMSO-$d^6$, 101 MHz, δ (ppm)): 166.55 (OCO), 138.56 (Ar–C–S), 133.19 (Ar–C–H), 131.55 (Ar–C–H), 131.44 (Ar–C–H), 126.03 (Ar–C–COO), 125.13 (Ar–C–H), 52.57 ($OCH_3$).

#### *2-Methylmercaptobenzoic acid methyl ester*

Sodium hydroxide (0.95 g, 23.75 mmol, 1.06 eq) was suspended in 20 ml methanol. The mixture was stirred while 2-mercaptobenzoic acid methyl ester (3.75 g, 22.30 mmol, 1 eq) was added. At 40 °C methyl iodide (3.25 g, 22.90 mmol, 1.02 eq) was added dropwise and the mixture became pale pink. The reaction mixture was heated to reflux for 2 h, then concentrated to one third of the total volume via distillation. 40 ml hot water was added to the residue provoking precipitation of a lightly pinkish solid. 2-Methylmercaptobenzoic acid methyl ester was isolated by filtration (3.983 g, 21.8 mmol, 98% of theory). $^1H$-NMR (DMSO-$d^6$, 400 MHz, δ (ppm)): 7.90 (dd, J = 7.9, 1.6 Hz, 1H, Ar–CH), 7.57 (td, J = 7.9, 1.6 Hz, 1H, Ar–CH), 7.38 (d, J = 8.1 Hz, 1H, Ar–CH), 7.28–7.17 (m, 1H, Ar–CH), 3.82 (s, 3H, OCH3), 2.42 (s, 3H, $SCH_3$). (Figure S8) $^{13}C$-NMR (DMSO-$d^6$, 101 MHz, δ (ppm)): 166.03 (OCO), 142.47 (Ar–C–S), 132.91 (Ar–C–H), 130.78 (Ar–C–H), 126.33 (Ar–C–COO), 124.87 (Ar–C–H), 123.71 (Ar–C–H), 52.06 ($OCH_3$), 14.79 ($SCH_3$). (Figure S9) IR (ATR, $\tilde{\nu}$ ($cm^{-1}$)): 2951 (vw), 2920 (vw), 1704 (w), 1584 (w), 1560 (w), 1461 (w), 1432 (w), 1304 (vw), 1285 (w), 1267 (w), 1245 (m), 1187 (w), 1144 (w), 1119 (vw), 1101 (w), 1059 (w), 1044 (w), 954 (w), 866 (vw), 825 (w), 798 (vw), 744 (m), 704 (w), 690 (w), 653 (w), 513 (w), 490 (w), 450 (w), 426 (vw), 409 (vw).

#### *2-Methylmercaptobenzohydroxamic acid (mmbHA)*

Hydroxylamine hydrochloride (11.670 g, 168 mmol, 4 eq) was dissolved in 250 ml water. Then sodium hydroxide (13.440 g, 336 mmol, 8 eq) was added. 2-Methylmercaptobenzoic acid methyl ester (7.654 g, 42 mmol, 1 eq), suspended in 110 ml 1,4-dioxane, was added dropwise to the clear solution. A colourless precipitate occurred. After 2 h of stirring the mixture became a clear solution again. Stirring was continued for 72 h. The clear light yellow solution was concentrated to one third of its volume, then acidified with 2 N hydrochloric acid to pH = 7. The solution was extracted five times with 25 ml ethyl acetate and washed with brine. The resulting colourless precipitate was filtered yielding **mmbHA** (1.792 g, 9.8 mmol). The organic layer was dried over magnesium sulfate and the solvent was removed to isolate further product (1.913 g, 10.5 mmol). (Combined isolated colorless solid **mmbHA** (3.705 g, 20.2 mmol, 48% of theory)) $^1H$-NMR (DMSO-$d^6$, 400 MHz, δ (ppm)): 10.90 (s, 1H, OH), 9.11 (s, 1H, NH), 7.53–7.39 (m, 1H, Ar–CH), 7.35 (d, J = 8.2 Hz, 1H, Ar–CH), 7.32–7.24 (m, 1H, Ar–CH), 7.17 (t, J = 7.4 Hz, 1H, Ar–CH), 2.40 (s, 3H, S–$CH_3$). (Figure S11) $^{13}C$-NMR (DMSO-$d^6$, 101 MHz, δ (ppm)): 164.91 (OCN), 138.01 (Ar–C–S), 133.17 (Ar–C–CON), 130.39 (Ar–CH), 127.71 (Ar–C–H), 125.78 (Ar–C–H), 124.22 (Ar–C–H), 15.25 ($SCH_3$). (Figure S12) IR (ATR, $\tilde{\nu}$ ($cm^{-1}$)): 3257 (vw), 3135 (vw), 2918 (w), 1743 (vw), 1677 (vw), 1608 (w), 1583 (w), 1561 (w), 1529 (w), 1461 (w), 1433 (w), 1414 (w), 1311 (w), 1286

Research Article
doi.org/10.1002/ejic.202200261



(vw), 1271 (vw), 1253 (w), 1233 (w), 1165 (w), 1131 (vw), 1076 (vw), 1063 (vw), 1043 (vw), 1026 (w), 974 (vw), 958 (vw), 898 (w), 742 (w), 708 (w), 697 (vw), 652 (w), 586 (w), 546 (w), 490 (w), 467 (w), 455 (vw). FD MS: $m/z = 182.97$ [mmbHA$^+$]

### *Complex Synthesis*

#### {Cu$^{II}$Cl$_2$(MeOH)[12-MC$_{Cu(II)N(mmbHA)}$-4]}$_2$·4MeOH (1)

**mmbHA** (111 mg, 0.61 mmol, 1 eq) was dissolved in 36 ml methanol. $CuCl_2$ (120 mg, 0.9 mmol, 1,5 eq) was added and the green solution was stirred overnight. Triethylamine (498 µL, 3.6 mmol, 6 eq) was added and stirring was continued for 2 h. After filtration the reaction mixture was left for slow evaporation (8 ml were used for layering experiments). Green crystals of compound **1** (20.1 mg, 0.04 mmol, 10% of theory (Cu)) could be isolated by filtration after one week. IR (ATR, $\tilde{\nu}$ (cm$^{-1}$)): 3384 (vw), 1630 (vw), 1573 (w), 1522 (w), 1471 (w), 1421 (w), 1369 (m), 1282 (w), 1261 (vw), 1154 (w), 1120 (vw), 1064 (w), 1043 (vw), 1012 (w), 976 (w), 946 (w), 929 (w), 913 (w), 769 (w), 734 (w), 693 (vw), 675 (w), 646 (w), 622 (w), 505 (w), 477 (w), 435 (w), 418 (w), 414 (w), 401 (vw). ESI MS: $m/z = 1075.69$ [MC$^{2+}$ + Cl$^-$]

#### {Cu$^{II}$($\mu_2$-ClO$_4$)(MeOH)$_2$(py)$_4$[12-MC$_{Cu(II)N(mmbHA)}$-4]}ClO$_4$ (2)

Manganese pivalate (111 mg, 0.4 mmol, 2 eq) and **mmbHA** (73 mg, 0.4 mmol, 2 eq) were stirred in 12 ml methanol. After adding pyridine (33 µL, 0.4 mmol, 2 eq), Cu(ClO$_4$)$_2$·6H2O (74 mg, 0.2 mmol, 1 eq) was added and the mixture was stirred for 3.5 h, filtered and left for slow evaporation. Filtration was repeated within the first week to keep a clear green solution. Green crystals of compound **2** (9.2 mg, 0.006 mmol, 14% of theory (Cu) were isolated by filtration after one week. IR (ATR, $\tilde{\nu}$ (cm$^{-1}$)): 3495 (vw), 2926 (vw), 2833 (vw), 1606 (w), 1590 (vw), 1567 (w), 1541 (w), 1486 (w), 1474 (w), 1446 (w), 1380 (w), 1326 (vw), 1282 (vw), 1261 (w), 1239 (vw), 1215 (vw), 1153 (vw), 1095 (m), 1070 (m), 1045 (w), 1017 (w), 968 (w), 926 (m), 770 (w), 758 (w), 740 (w), 696 (m), 666 (w), 643 (w), 622 (m), 580 (w), 495 (w), 476 (w), 443 (vw), 431 (vw), 419 (w), 407 (vw). $^1$H-NMR (DMSO-d$^6$, 400 MHz, δ (ppm)): 14.28 (s, 3H), 9.38 (s, 3H), 7.67 (d, J = 95.6 Hz, 3H), 4.60 (s, 2H), 4.11 (s, 1H), 3.16 (s, 3H). ESI MS: $m/z = 520.36$ [MC$^{2+}$].

Deposition Numbers 2160754 (for **1**) and 2160755 (for **2**) contain the supplementary crystallographic data for this paper. These data are provided free of charge by the joint Cambridge Crystallographic Data Centre and Fachinformationszentrum Karlsruhe Access Structures service www.ccdc.cam.ac.uk/structures.

## *Acknowledgements*

*The authors express their gratitude to Dr. Dieter Schollmeyer for valuable discussions and for performing the XRD studies. CG kindly acknowledges the Excellence Initiative by the Graduate School of Excellence Materials Science in Mainz, Germany (DFG/GSC 266). Open Access funding enabled and organized by Projekt DEAL.*

## *Conflict of Interest*

The authors declare no conflict of interest.

## Data Availability Statement

The data that support the findings of this study are available from the corresponding author upon reasonable request.

**Keywords:** Coordination Chemistry · Copper(II) · Ion selectivity · Ligand · Metallacrown

[1] M. S. Lah, V. L. Pecoraro, *J. Am. Chem. Soc.* **1989**, *111*, 7258–7259.
[2] A. Rauguth, A. Kredel, L. M. Carrella, E. Rentschler, *Inorg. Chem.* **2021**, *60*, 14031–14037.
[3] M. Ostrowska, I. O. Fritsky, E. Gumienna-Kontecka, A. V. Pavlishchuk, *Coord. Chem. Rev.* **2016**, *327–328*, 304–332.
[4] J. J. Bodwin, A. D. Cutland, R. G. Malkani, V. L. Pecoraro, *Coord. Chem. Rev.* **2001**, *216–217*, 489–512.
[5] G. Mezei, C. M. Zaleski, V. L. Pecoraro, *Chem. Rev.* **2007**, *107*, 4933–5003.
[6] P. Happ, C. Plenk, E. Rentschler, *Coord. Chem. Rev.* **2015**, *289–290*, 238–260.
[7] A. Lüpke, L. M. Carrella, E. Rentschler, *Chem. Eur. J.* **2021**, *27*, 4283–4286.
[8] P. Happ, E. Rentschler, *Dalton Trans.* **2014**, *43*, 15308–15312.
[9] A. J. Lewis, E. Garlatti, F. Cugini, M. Solzi, M. Zeller, S. Carretta, C. M. Zaleski, *Inorg. Chem.* **2020**, 59, 11894–11900.
[10] D. M. Griffith, A. Haughey, S. Chahal, H. Müller-Bunz, C. J. Marmion, *Inorg. Chim. Acta* **2010**, *363*, 2333–2337.
[11] D. Gaynor, Z. A. Starikova, W. Haase, K. B. Nolan, *J. Chem. Soc. Dalton Trans.* **2001**, 1578–1581.
[12] D. Gaynor, Z. A. Starikova, S. Ostrovsky, W. Haase, K. B. Nolan, *Chem. Commun.* **2002**, 506–507.
[13] A. A. Athanasopoulou, C. Gamer, L. Völker, E. Rentschler, *Novel Magnetic Nanostructures: Unique Properties and Applications* **2018**,1st Edition, Elsevier, ISBN: 9780128135945.
[14] N. F. Chilton, R. P. Anderson, L. D. Turner, A. Soncini, K. S. Murray, *J. Comput. Chem.* **2013**, *34*, 1164–1175.
[15] A. V. Pavlishchuk, S. V. Kolotilov, M. Zeller, O. V. Shvets, I. O. Fritsky, S. E. Lofland, A. W. Addison, A. D. Hunter, *Eur. J. Inorg. Chem.* **2011**, *2011*, 4826–4836.
[16] C. McDonald, T. Whyte, S. M. Taylor, S. Sanz, E. K. Brechin, D. Gaynor, L. F. Jones, *CrystEngComm* **2013**, *15*, 6672–6681.
[17] Y. Song, J. C. Liu, Y. J. Liu, D. R. Zhu, J. Z. Zhuang, X. Z. You, *Inorg. Chim. Acta* **2000**, *305*, 135–142.
[18] F. Cao, R. M. Wei, J. Li, L. Yang, Y. Han, Y. Song, J. M. Dou, *Inorg. Chem.* **2016**, *55*, 5914–5923.
[19] G. A. Bain, J. F. Berry, *J. Chem. Educ.* **2008**, *85*, 532–536.
[20] G. M. Sheldrick, *Acta Crystallogr.* **2015**, *71*, 3–8.
[21] G. M. Sheldrick, T. R. Schneider, *Methods Enzymol.* **1997**, *277*, 319–343.
[22] O. v. Dolomanov, L. J. Bourhis, R. J. Gildea, J. A. K. Howard, H. Puschmann, *J. Appl. Crystallogr.* **2009**, *42*, 339–341.

Manuscript received: April 25, 2022
Revised manuscript received: May 18, 2022
Accepted manuscript online: May 25, 2022